

Thermoanalytical behaviour of histidine complexes with transition metal ions

S. Materazzi *, R. Curini, G. D'Ascenzo

Department of Chemistry, University "La Sapienza", Rome, Italy

Received 21 February 1995; accepted 10 August 1995

Abstract

The tendency of histidine to form biologically important complexes with transition metal ions is well known. However, in the literature there is little information about the thermochemical behaviour of these complexes in the solid state, and the results are often contradictory.

In this work, the synthesis and the thermoanalytical investigation of complexes of formula MeHis_2 , $\text{MeHis}_2(\text{NO}_3)_2$ and $\text{MeHis}_6(\text{NO}_3)_2$ are reported, with $\text{Me} = \text{Co(II)}$, Ni(II) or Cu(II) and $\text{His} = \text{histidine}$.

The results show anomalous behaviour for histidine as a ligand compared with imidazole and its derivatives, in metal–ligand–nitrate ion interactions.

Keywords: Complexes; DSC; DTG; Histidine; TG–FTIR

1. Introduction

Histidine is a fundamental amino acid for living organisms: it is present in the structural configuration of many enzymes and metalloproteins such as carbonic oxidoreductase [1], carboxipeptidase [2], thermolysine [3], etc., and in many biologically active molecules, such as the plasmatic tripeptide glycyl–l–istidyl–l–lysine known as a growth modulator [4].

Histidine can also act as a biological carrier for oxygen because its complexes with transition metal ions can reversibly bind oxygen in aqueous solutions [5–7]. Moreover, the imidazolic ring of histidine is a ligand for transition metal ions in molecules such as heme or vitamin B_{12} [8]. In human serum histidine tends to bind Cu(II) ions, and also readily forms complexes with Co(II) and Ni(II) ions.

* Corresponding author.

The study of the interactions between histidine and transition metal ions such as Co(II), Ni(II) and Cu(II) is, therefore, very interesting because the molecule's bioactivity changes with changing pH or metal/ligand ratio.

This work reports the synthesis and thermoanalytical behaviour of the complexes MeHis₂, MeHis₂(NO₃)₂ and MeHis₆(NO₃)₂ with Me = Co(II), Ni(II) and Cu(II).

2. Experimental

2.1. Synthesis of the complexes

The synthesis of MeHis₂ complexes was carried out by adding Me(NO₃)₂ solution to histidine solution at a ratio of 1:2 and with the pH around that of histidine p*K*_{a1} - adjusting it with HNO₃. The precipitate was then washed and dried in vacuo.

Evertsson [9] obtained CuHis₂(NO₃)₂·2H₂O in the solid state from solutions of histidine and CuSO₄ at a 2:1 ratio and an excess of NaNO₃. We initially followed this method but the precipitates were always mixtures of complexes. So, to obtain complexes of general formula MeHis_x(NO₃)₂, with Me = Co(II), Ni(II) or Cu(II), an aqueous solution of histidine was acidified at pH < 1 with HNO₃, and then the Me(NO₃) solution was added in stoichiometric ratio.

To favour the formation of complexes, the solution were heated before mixing, leaving the final solution in a closed vessel. If the complex did not precipitate, a 1:1 ethanol–diethyl ether solution was added portionwise to furnish an oil and then an hygroscopic solid-state complex.

2.2. Instrumentation

Thermoanalytical curves were obtained using a Perkin–Elmer TGA7 thermobalance for low temperatures (range 20–1000°C) and a Perkin–Elmer DSC7. The atmosphere was argon, nitrogen or air, with a flow rate of 50–100 cm³ min⁻¹. The heating rate was varied between 5 and 40°C min⁻¹.

The thermobalance was coupled with a Perkin–Elmer FTIR, model 1760X, to obtain the IR spectra of gases evolved during the thermogravimetric analysis. The TGA7 was coupled to the heated gas cell of the FTIR instrument by means of a heated transfer line.

Gaseous or vaporised components were flushed by a suitable gas and the temperatures of the cell and of the transfer line independently selected. The only materials in contact with the sample gases were the PTFE of the transfer line, KBr of the cell windows and the glass of the TGA7 furnace.

3. Results

The TG curves of the MeHis₂ complexes (Figs. 1–3) show two main regions of weight loss. The first, located in the range 180–400°C, is the convolution of at least two

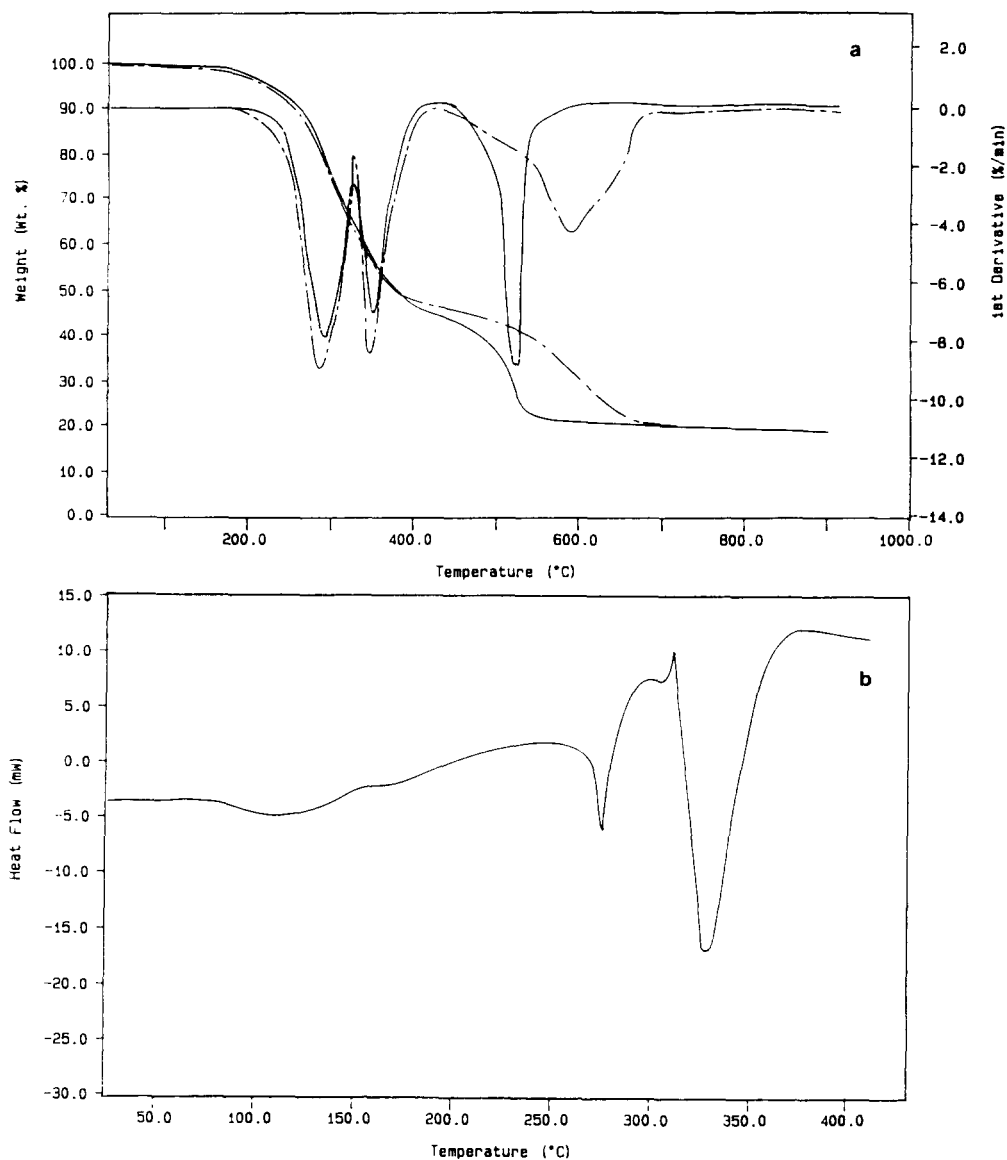


Fig. 1. CoHis_2 : (a) TG and DTG curves: — air — — nitrogen; (b) DSC curve (open capsule); scanning rate $10^\circ\text{C min}^{-1}$; flow rate $50\text{--}100\text{ ml min}^{-1}$.

processes, as can be seen from the related DTG curves, while the second process, in the range $430\text{--}570^\circ\text{C}$ leads to the production of metal oxide.

Figs. 4–6 show the thermal decomposition of the $\text{MeHis}_2(\text{NO}_3)_2$ complexes; this happens in two processes, the first in the interval $90\text{--}190^\circ\text{C}$, the second in the range $311\text{--}370^\circ\text{C}$ for the Co(II) complex, $320\text{--}385^\circ\text{C}$ for the Cu(II) complex, and $330\text{--}410^\circ\text{C}$ for the Ni(II) complex.

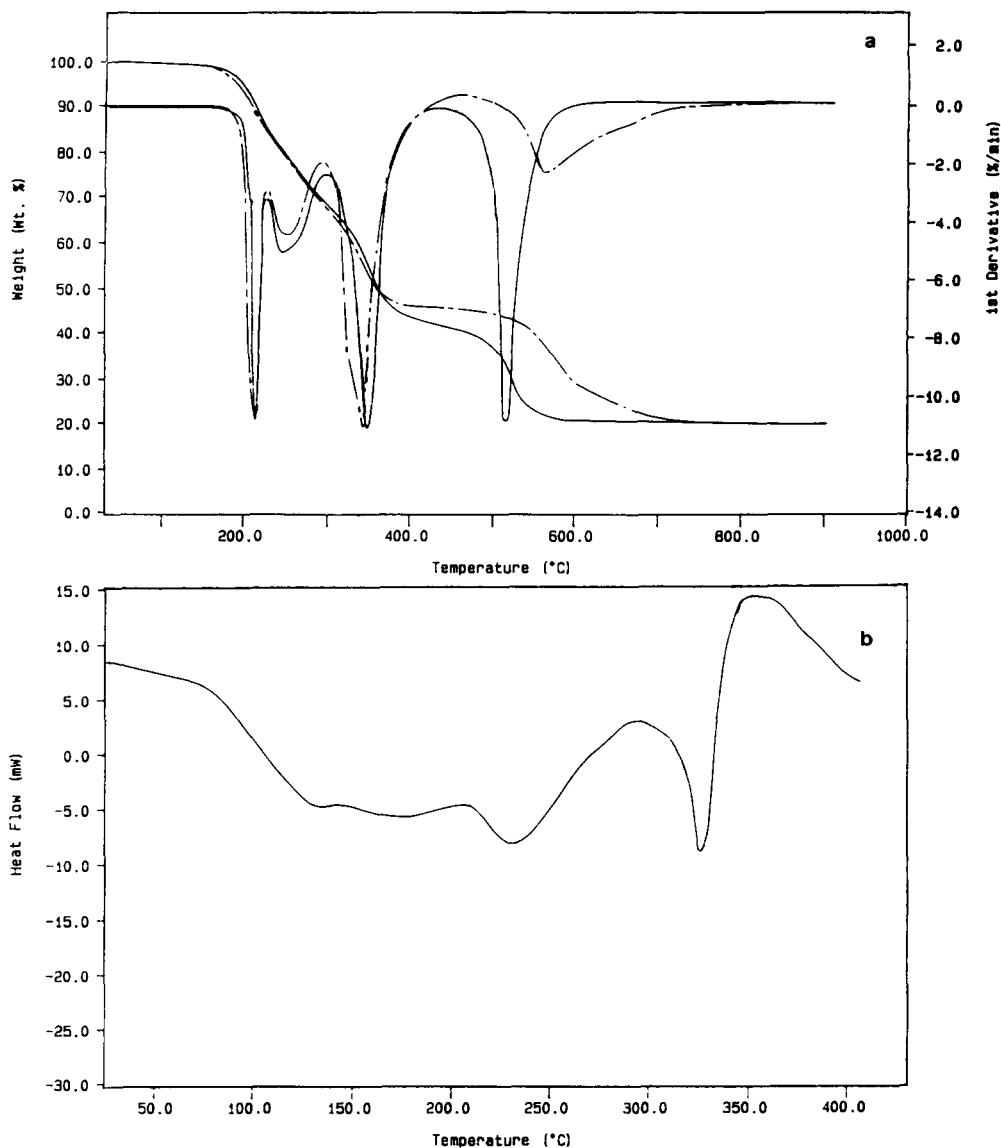


Fig. 2. NiHis_2 : (a) TG and DTG curves: — air — — — nitrogen; (b) DSC curve (open capsule); scanning rate $10^{\circ}\text{C min}^{-1}$; flow rate $50\text{--}100\text{ ml min}^{-1}$.

The thermal behaviour of the $\text{MeHis}_6(\text{NO}_3)_2$ complexes is shown in Figs. 7–9. In the TG and DTG curves two main processes are present: the first is located in the range $120\text{--}190^{\circ}\text{C}$ for the Ni(II) and Cu(II) complexes, while for the Co(II) complex the interval is $160\text{--}220^{\circ}\text{C}$; the second process, in the range $300\text{--}500^{\circ}\text{C}$, produces the metal oxide.

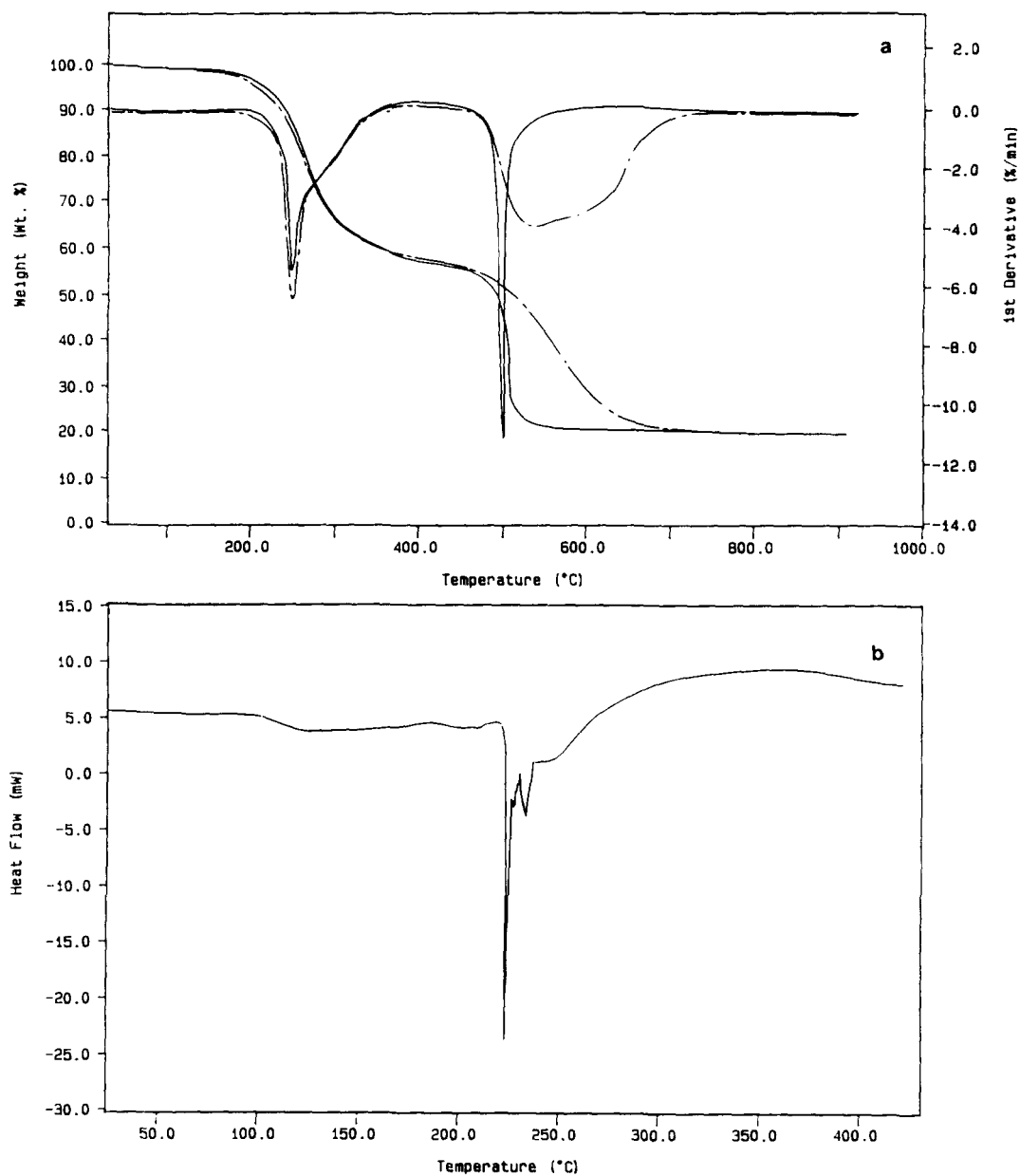


Fig. 3. CuHis_2 : (a) TG and DTG curves: — air — — nitrogen; (b) DSC curve (open capsule); scanning rate $10^{\circ}\text{C min}^{-1}$; flow rate: $50\text{--}100\text{ ml min}^{-1}$.

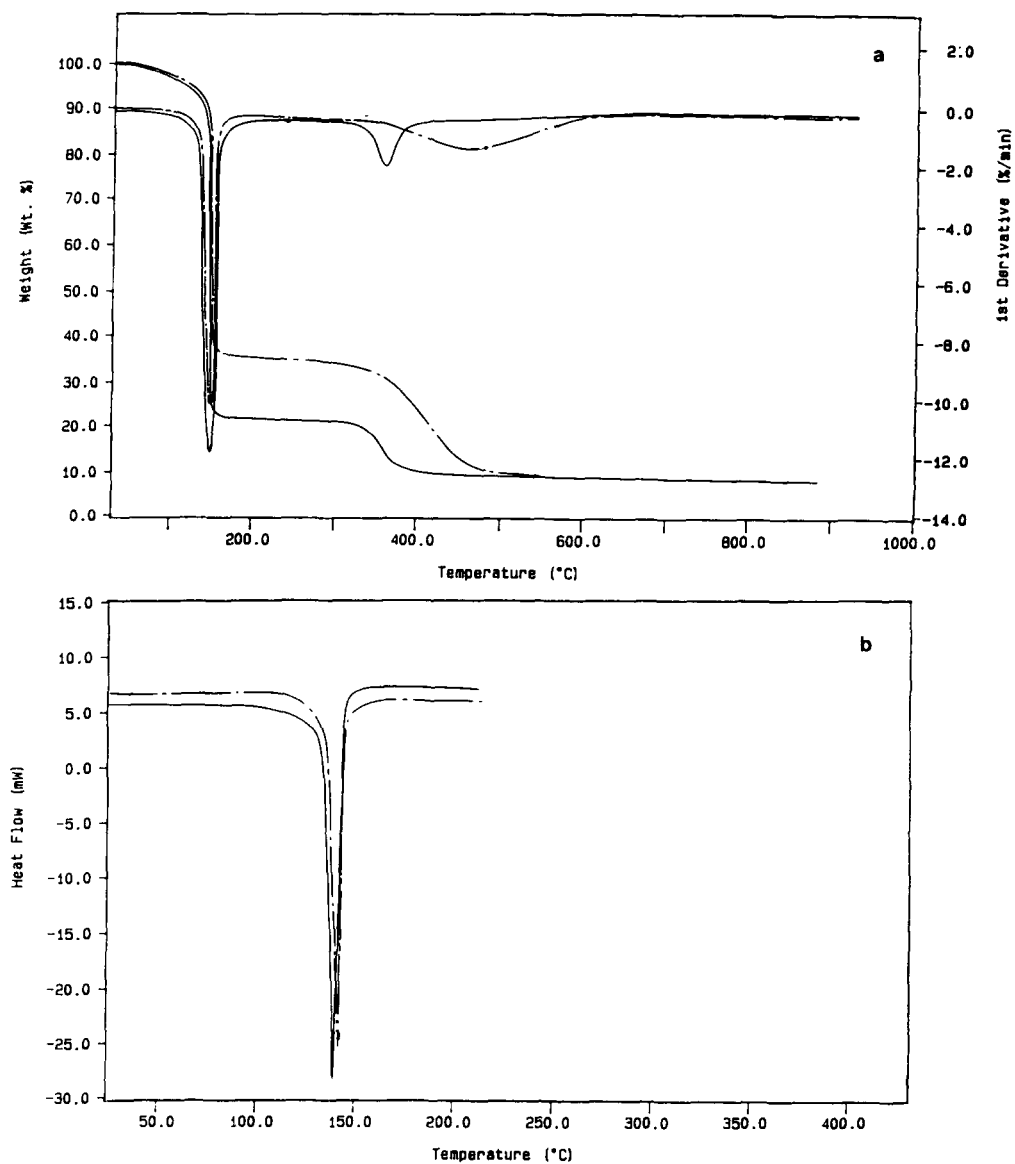


Fig. 4. $\text{CoHis}_2(\text{NO}_3)_2$: (a) TG and DTG curves: — air — — nitrogen; (b) DSC curve: — open capsule — — closed capsule; scanning rate $10^{\circ}\text{C min}^{-1}$; flow rate $50\text{--}100\text{ ml min}^{-1}$.

4. Discussion

The complexes of histidine with transition metal ions can be assumed to be relatively simple models for studying the mechanisms of action of some biologically important

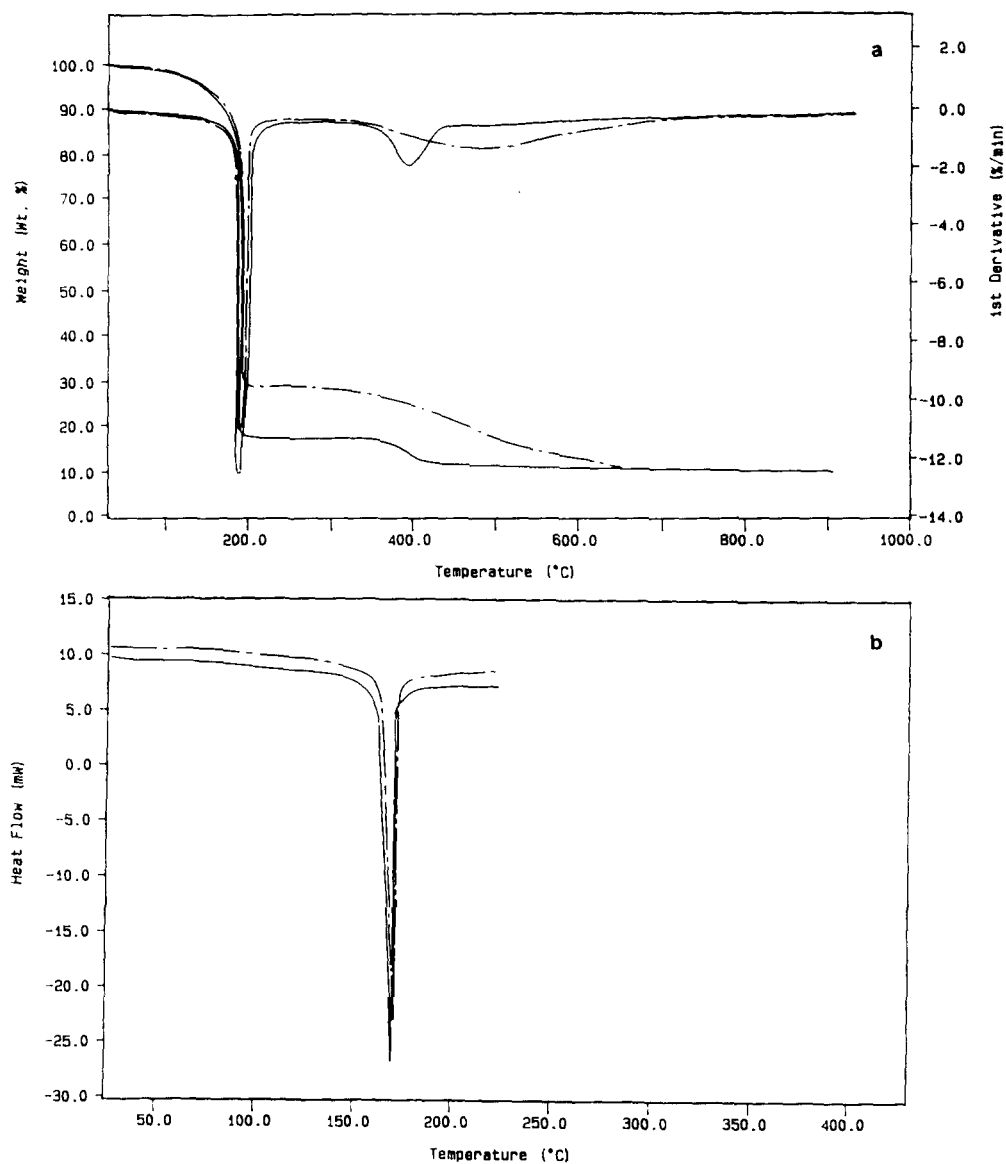


Fig. 5. $\text{NiHis}_2(\text{NO}_3)_2$: (a) TG and DTG curves: — air — nitrogen; (b) DSC curve: — open capsule — closed capsule; scanning rate $10^{\circ}\text{C min}^{-1}$; flow rate $50\text{--}100\text{ ml min}^{-1}$.

enzymes and for explaining many oxygen-transport mechanisms, in which histidine interacts through a metal-catalyzed reaction.

Histidine presents characteristic behaviour because of its four potential coordination sites: the carboxylic group, the pyridinic nitrogen, the amino group, and the

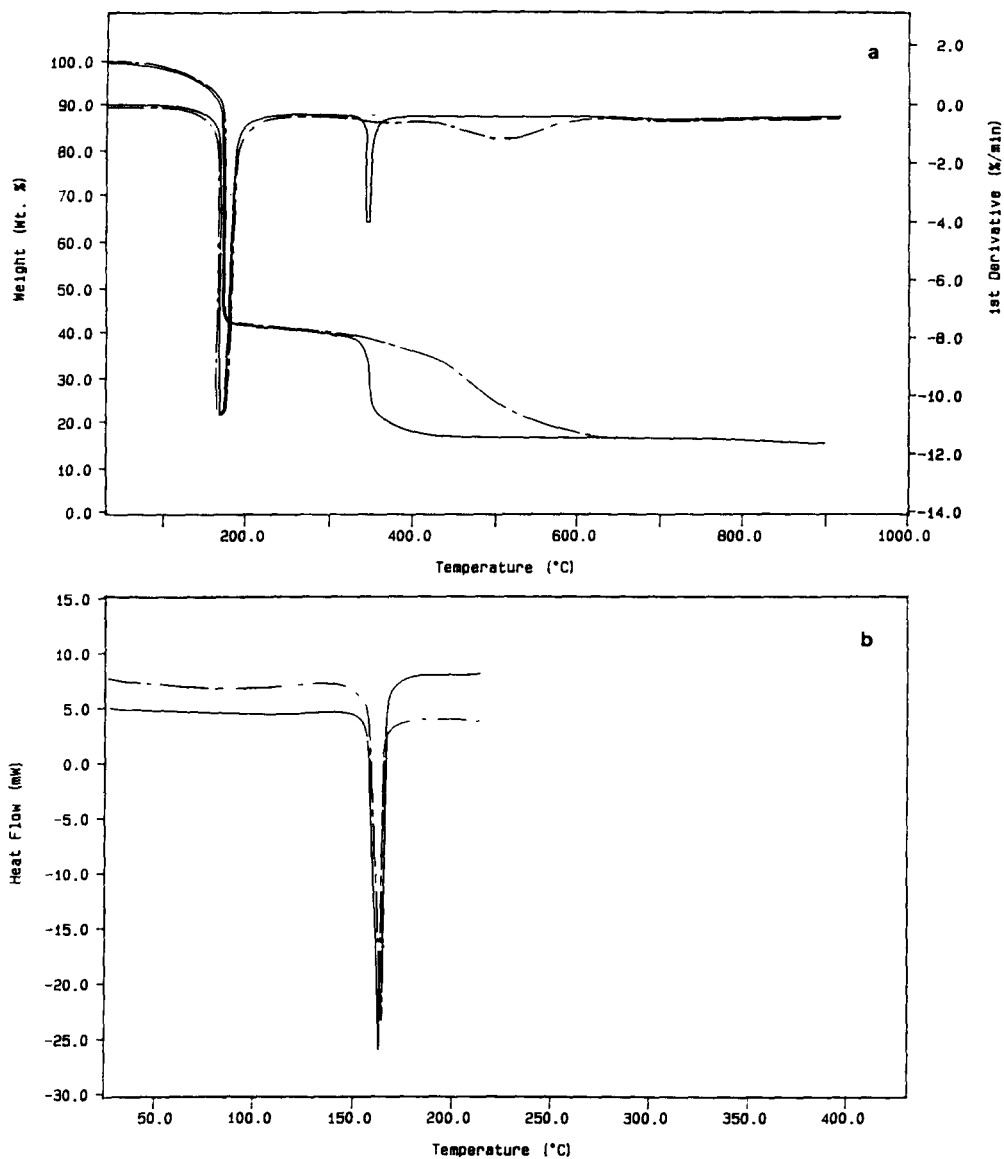


Fig. 6. $\text{CuHis}_2(\text{NO}_3)_2$: (a) TG and DTG curves: — air — — nitrogen; (b) DSC curve: — open capsule — — closed capsule; scanning rate $10^{\circ}\text{C min}^{-1}$; flow rate $50\text{--}100\text{ ml min}^{-1}$.

pyrrolic nitrogen. From X-ray studies [10], it has been demonstrated that histidine can use only three of the four coordination sites to bind transition metal ions; ions with an octahedral coordination geometry can bind histidine as tridentate ligand. Crystallographic data show that histidine can act as a bidentate ligand with the amino-

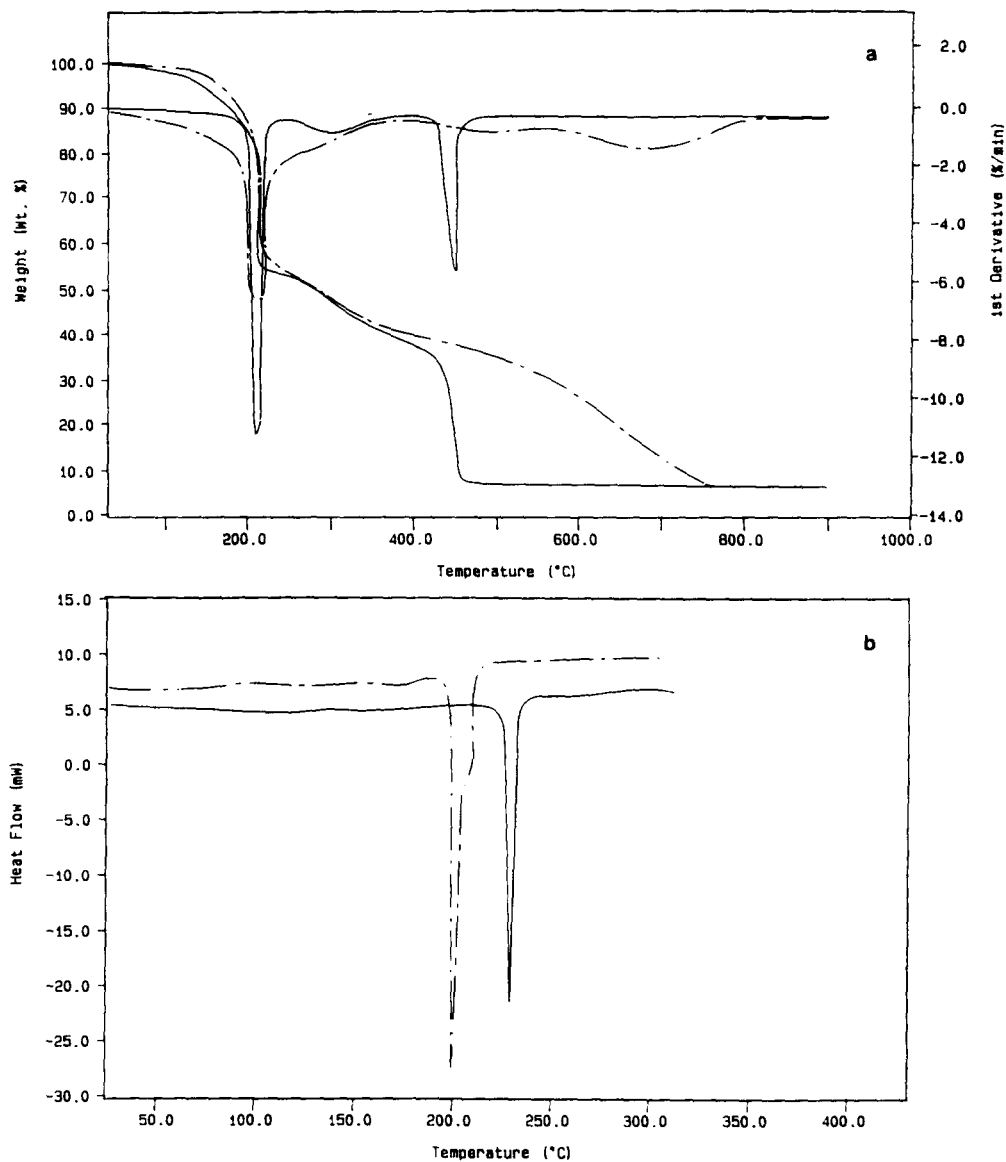


Fig. 7. $\text{CoHis}_6(\text{NO}_3)_2$: (a) TG and DTG curves: — air — — nitrogen; (b) DSC curve: — open capsule — — closed capsule; scanning rate $10^{\circ}\text{C min}^{-1}$; flow rate $50\text{--}100\text{ ml min}^{-1}$.

imidazolic couple or with the amino-carboxylated couple, while the third possible couple (imidazolic-carboxylated) is not favoured by the formation of a seven-membered ring. The values of the stability constants of histidine with divalent metal ions are reported in Table 1; Table 2 shows $-\Delta H_f$ values for the MeHis_2 compounds.

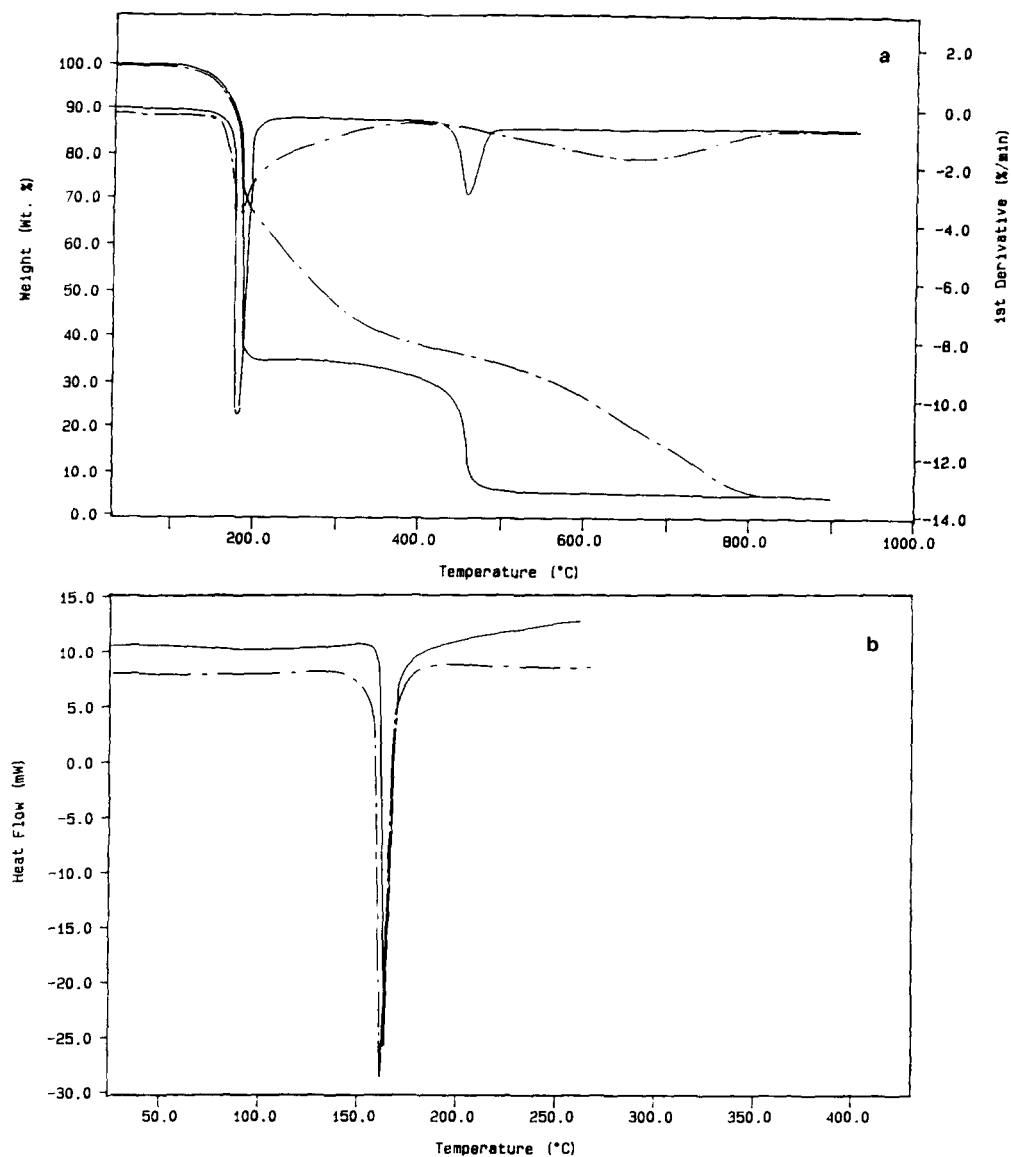


Fig. 8. $\text{NiHis}_6(\text{NO}_3)_2$: (a) TG and DTG curves: — air — nitrogen; (b) DSC curve: — open capsule — closed capsule; scanning rate $10^{\circ}\text{C min}^{-1}$; flow rate $50\text{--}100\text{ ml min}^{-1}$.

Although many workers have studied the interactions between histidine and transition metal ions, there is not much information about the thermochemical characteristics of these complexes in the solid state, and often the results are not in agreement.

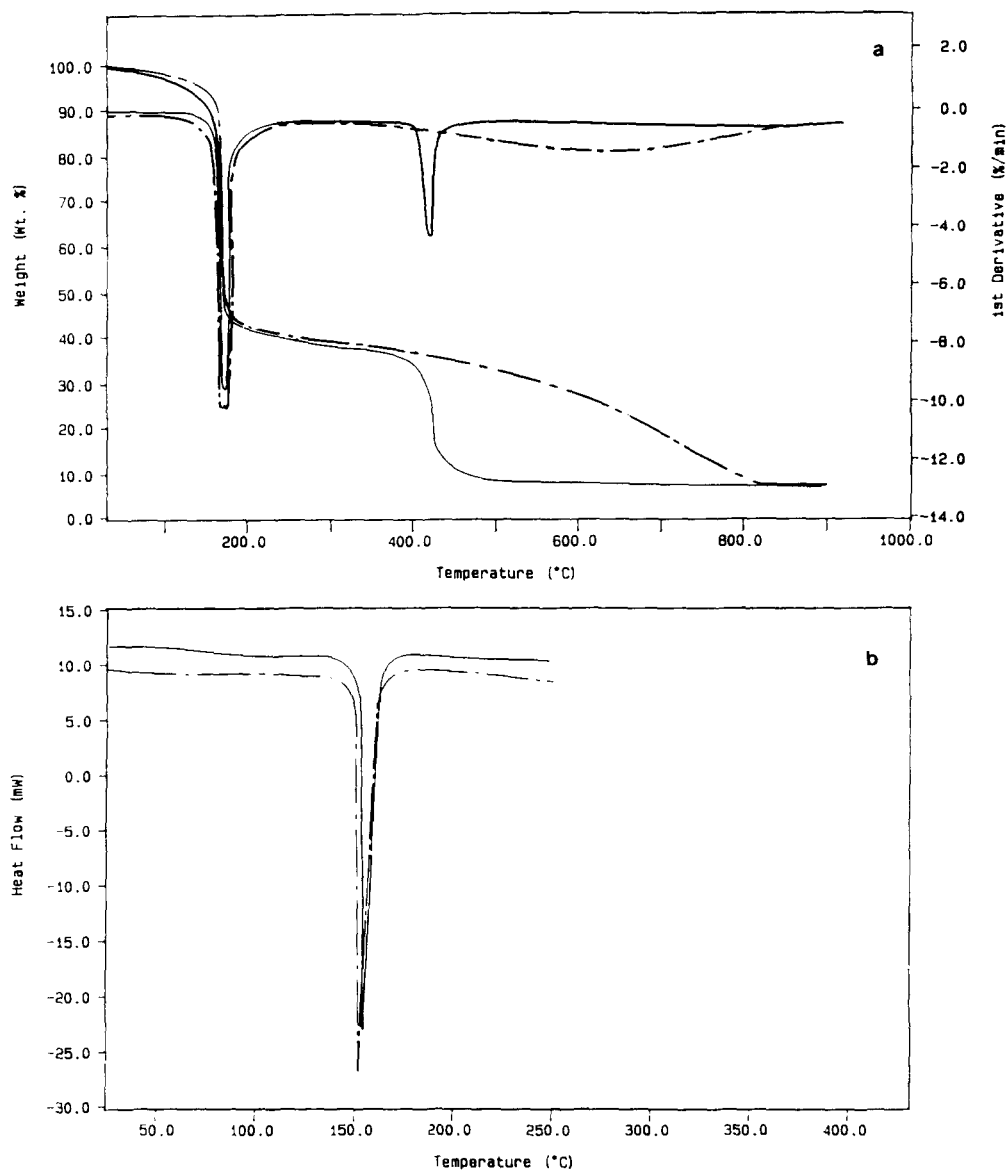


Fig. 9. $\text{CuHis}_6(\text{NO}_3)_2$: (a) TG and DTG curves: — air — — nitrogen; (b) DSC curve: — open capsule — — closed capsule; scanning rate $10^{\circ}\text{C min}^{-1}$; flow rate $50\text{--}100\text{ ml min}^{-1}$.

TG curves for MeHis_2 compounds show that in the first decomposition step the behaviour is the same with either oxidative or inert gas flow, and two overlapping processes are always present; the second, final process, to give metal oxide occurs in a lower range in air than under nitrogen or argon flow. The corresponding DSC curves

Table 1
Stability constants of histidine–divalent metal ion complexes

| | | H^+ | Co(II) | Ni(II) | Cu(II) |
|-------------------|-------|-------|--------|--------|--------|
| 4-Methylimidazole | K_1 | 7.69 | – | – | 4.13 |
| | K_2 | – | – | – | 3.49 |
| | K_3 | – | – | – | 2.87 |
| | K_4 | – | – | – | 2.00 |
| Imidazole | K_1 | 7.11 | 2.45 | 3.00 | 4.20 |
| | K_2 | – | 1.90 | 2.50 | 3.42 |
| | K_3 | – | 1.40 | 2.00 | 2.88 |
| | K_4 | – | – | 1.50 | 2.10 |
| Histidine | K_1 | 9.15 | 6.90 | 8.70 | 10.10 |
| | K_2 | 6.10 | 5.50 | 6.90 | 8.00 |

Table 2
Enthalpies of formation ($-\Delta H_f/(\text{kJ mol}^{-1})$) of MeHis₂ compounds

| Co(II) | Ni(II) | Cu(II) | Ref. |
|--------|--------|--------|------|
| – | 16.2 | 21.0 | [11] |
| – | 16.6 | 21.3 | [12] |
| – | 16.5 | 20.0 | [13] |
| – | – | 21.3 | [14] |
| 9.6 | 13.6 | 22.1 | [15] |
| 12.3 | 18.9 | 20.1 | [16] |

confirm the two overlapping exothermic processes in the first decomposition step; these are not correlated with structural modifications but only with oxidative processes.

So, a first decomposition step can be assumed in which the carboxylic group of the histidine decomposes to give carbondioxide; the further process gives an oxidative decomposition in air flow or a distillation and non-oxidative thermodecomposition in inert gas flow (nitrogen or argon).

FTIR spectra of the evolved gas (Fig. 10) support this hypothesis, showing for the first process the characteristic bands of CO₂ only at 2358–2343 cm⁻¹, and for the successive processes the bands of CO₂ and the doublet at 966–931 cm⁻¹ due to the loss of amino groups.

Our results agree with the structures reported in the literature for bis-histidino Co(II) and bis-histidino Ni(II) complexes [10, 17]. The metal interacts with the ligand through the amino nitrogen, the carboxylic group and the pyridinic nitrogen, while two oxygen atoms of two carboxylic groups interact with the central ion (Fig. 11).

Infrared spectra of the MeHis₂ complexes show strong bands in the range 3371–3132 cm⁻¹ (ν_{as} and ν_s for N–H) and 1628–1398 cm⁻¹ (ν_{as} and ν_s for COO⁻) as reported in Table 3.

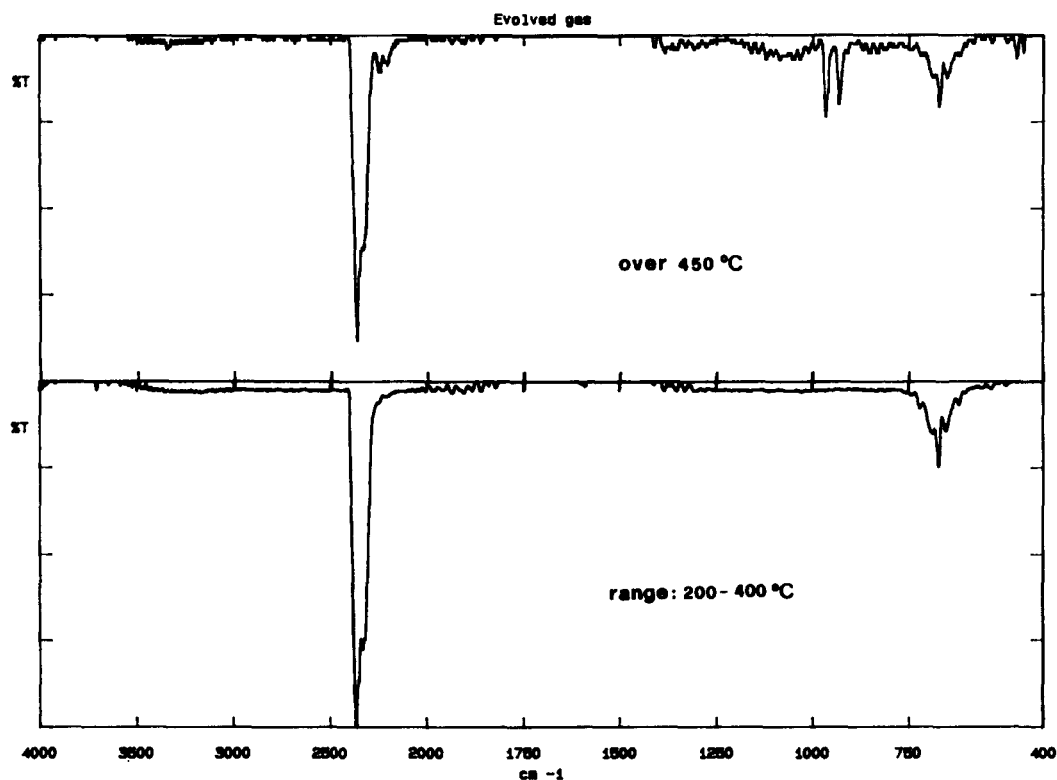


Fig. 10. Infrared spectra of the evolved gases for the MeHis₂ complexes.

The COO⁻ frequencies change in the same manner as for N–H, and the absence of COO⁻ bands around 1725 cm⁻¹ points to the ionic character of the metal–carboxyl group band.

From these results, we propose the stability scale



in agreement with Irving and Williams [18]. This thermal stability scale is exactly the opposite of that verified for other coordination compounds [19–21]:



and it is interesting to note that the CoHis₂ complex is more stable than the NiHis₂ one, while normally other ligands give Co(II) and Ni(II) complexes with comparable stability. The TG curves of MeHis₂(NO₃)₂ complexes show a thermoanalytical profile with two main processes, the first being almost explosive even under nitrogen or argon flow. The thermal decomposition to metal oxide occurs in a second process that is percentually higher if the atmosphere is inert and if the Co(II) complex is compared with those of Ni(II) or Cu(II).

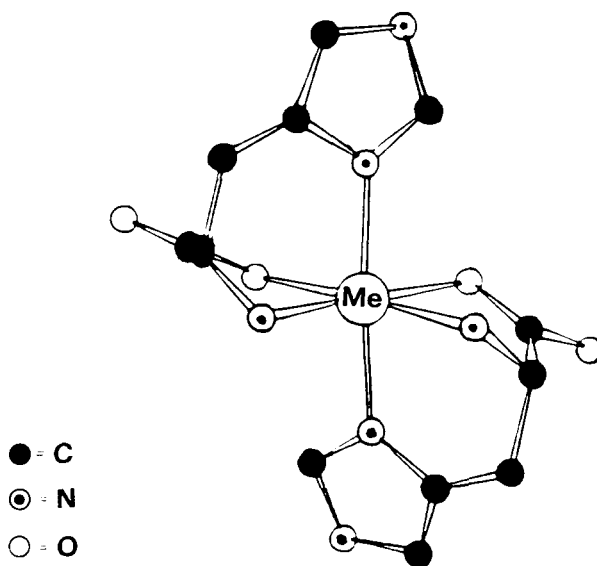


Fig. 11. Structure of bis-histidino complexes.

Table 3
Band frequencies of MeHis₂ complexes

| | CoHis ₂ | NiHis ₂ | CuHis ₂ |
|--|--------------------|--------------------|--------------------|
| $\nu_{as} \text{NH}/\text{cm}^{-1}$ | 3371 | 3307 | 3300 |
| $\nu_s \text{NH}/\text{cm}^{-1}$ | 3221 | 3161 | 3132 |
| $\nu_{as} \text{COO}^-/\text{cm}^{-1}$ | 1628 | 1601 | 1590 |
| $\nu_s \text{COO}^-/\text{cm}^{-1}$ | 1404 | 1398 | 1393 |

The TG curves of pure histidine, of histidine–nitrate synthetic mixtures and of NaNO₃ show very different profiles. Thus, the first exothermic process must be an oxidation process of the complex probably due to the interaction of the nitrate ion with the ligand catalyzed by the central ion. The DSC curves support this hypothesis in comparing the onset temperatures and the ΔH values in the case of scans either with open capsule and N₂ flow or with closed capsule (Table 4).

The closed capsule keeps the exhaust gases in contact with the samples, so lowering the decomposition temperatures and raising the ΔH values.

Concerning the IR bands, the MeHis₂(NO₃)₂ complexes show a strong band at 1047 cm⁻¹ and two bands at 1405 and 1324 cm⁻¹ assigned to the split frequencies due to the lowering of the nitrate symmetry. The N–H and COO⁻ bands are comparable with those of the MeHis₂ complexes. The results suggest octahedral coordination with the nitrate apically coordinated, and with the carboxylic group and the amino group in the metal plane.

Table 4
 ΔH and onset temperatures

| | $\Delta H/(\text{Kcal mol}^{-1})$ | | Onset temperature/ $^{\circ}\text{C}$ | |
|--|-----------------------------------|----------------|---------------------------------------|----------------|
| | N_2 | Closed capsule | N_2 | Closed capsule |
| CoHis ₂ | – 26.75 | | 270.3 | |
| NiHis ₂ | – 34.23 | | 212.1 | |
| CuHis ₂ | – 36.15 | | 211.0 | |
| CoHis ₂ (NO ₃) ₂ | – 177.20 | – 232.92 | 137.0 | 132.0 |
| NiHis ₂ (NO ₃) ₂ | – 181.59 | – 217.14 | 167.2 | 165.9 |
| CuHis ₂ (NO ₃) ₂ | – 191.55 | – 204.48 | 160.7 | 159.2 |
| CoHis ₆ (NO ₃) ₂ | – 132.43 | – 301.61 | 196.4 | 197.4 |
| NiHis ₆ (NO ₃) ₂ | – 146.01 | – 284.71 | 162.8 | 161.1 |
| CuHis ₆ (NO ₃) ₂ | – 147.50 | – 209.99 | 153.7 | 150.7 |

The thermal behaviour of the MeHis₆(NO₃)₂ complexes is similar to that of the MeHis₂(NO₃)₂ ones, with two processes, the first of which very exothermic for the Ni(II) and the Cu(II) complexes, and slightly less violent for that of Co(II); the flow, whether oxidant or inert, has little influence on this first process. The second process gives the metal oxides.

With regard to the MeHis₂(NO₃)₂ complexes, the DSC curves show an exothermic peak either in air or in nitrogen or argon flow, corresponding to the first TG process, and the temperatures are lower if a closed capsule is used; conversely, the ΔH values are higher than the open capsule values, so a metal-catalyzed oxidation reaction can again be supposed.

The IR bands at 1047 cm^{–1} (strong) and at 1405–1324 cm^{–1} seen for the MeHis₂(NO₃)₂ complexes are still present; the presence of a coordinated nitrate when six histidine molecules are present can be explained by an Me(His)₂–(His)₄(NO₃)₂ system and would imply the presence of two processes in the TG curve, one for the loss of four histidine molecules and the other for that of the last two. In fact, the TG curve of the CoHis₆(NO₃)₂ complex, with nitrogen flow, shows an initial non-violent process that becomes exothermic a few degrees later. The initial loss is due to the four histidine molecules, but the oxidative process masks the two theoretical decomposition steps. In the case of Ni(II) and Cu(II) compounds, the oxidative process completely covers the initial loss also.

The thermal profile of the studied compounds enhances the anomalous behavior of histidine as a ligand compared with imidazole or its derivatives; in fact, only histidine shows exothermic reactions also in nitrogen atmosphere due to the metal–ligand–nitrate ion interaction.

Acknowledgement

Financial support by Grants (40 and 60%) from MURST, Italy is gratefully acknowledged.

References

- [1] A. Liljas, K.K. Kannan, P.C. Bergstein and I. Waara, *Nature* (London), 235 (1972) 131.
- [2] W.N. Lipscomb, J.A. Hartsuck, F.A. Quiocho and G.N. Reeke Jr., *Proc. Natl. Acad. Sci. USA*, 64 (1969) 28.
- [3] B.W. Matthews, J.N. Jansonius, P.M. Colman and B.P. Schoenhom, *Nature* (London), 238 (1972) 41.
- [4] L. Pickart, W.H. Goodwin, W. Burga, T.B. Murphy and D.K. Johnson, *Biochem. Pharmacol.*, 32 (1983) 3868.
- [5] D. Burk, J.Z. Heason, L. Caroline and A.L. Schade *J. Biol. Chem.*, 165 (1946) 723.
- [6] D. Burk, J.Z. Heason, H.B. Levy and A.L. Schade, *Fed. Proc.*, 6 (1947) 242.
- [7] C.C. McDonald and W.D. Phillips, *J. Am. Chem. Soc.*, 85 (1963) 3736.
- [8] R.J. Sundberg and R.B. Martin, *Chem. Rev.*, 74 (1974) 4.
- [9] B. Evertsson, *Acta Crystallogr. Sect B*: 25 (1969) 30.
- [10] M.M. Harding and H.A. Long, *J. Chem. Soc. A*: (1968) 2554.
- [11] A.C.R. Thornton and H.A. Skinner, *Trans. Faraday Soc.*, 65 (1969) 2044.
- [12] W.F. Stack and H.A. Skinner, *Trans. Faraday Soc.*, 63 (1967) 1136.
- [13] D.S. Barnes and L.D. Peltit, *J. Inorg. Nucl. Chem.*, 33 (1971) 2177.
- [14] J.L. Meyer and J.E. Baumann, *J. Am. Chem. Soc.*, 92 (1970) 4210.
- [15] E.V. Raju and H.B. Mathur, *J. Inorg. Nucl. Chem.*, 31 (1969) 425.
- [16] D.R. Williams, *J. Chem. Soc. A*: (1970) 1550.
- [17] K.A. Fraser and M.M. Harding, *J. Chem. Soc. A*: (1967) 415.
- [18] R. Irving and J.P. Williams, *J. Chem. Soc.*, (1953) 3192.
- [19] G. D'Ascenzo, U. Biader Cepidor and G. De Angelis, *Anal. Chim. Acta*, 58 (1972) 175.
- [20] R. Curini, S. Materazzi, G. D'Ascenzo and G. De Angelis, *Thermochim. Acta*, 161 (1990) 297.
- [21] R. Curini, S. Materazzi and G. D'Ascenzo, *Thermochim. Acta*, 164 (1990) 237.